Passive mode-locking using phase-sensitive amplification

J. Nathan Kutz*
Department of Applied Mathematics, University of Washington, Seattle, Washington 98195-2420, USA
(Received 12 May 2008; published 30 July 2008)

A method is proposed and considered theoretically for using phase-sensitive amplification as the intensity-discrimination (saturable absorption) element in a laser cavity to generate stable and robust mode-locking. The phase-sensitive amplifier acts as a phase filter for selecting the specific intensity-dependent phase rotation of the mode-locked pulse that locks the phase to the amplifier pump phase. The nonlinear phase rotation is analogous to the nonlinear polarization rotation which is used with passive polarizers for mode-locking. It is demonstrated that the phase-sensitive amplification mechanism can indeed result in stable mode-locking. An average cavity model explicitly calculates the stability of the mode-locked pulses.

DOI: 10.1103/PhysRevA.78.013845 PACS number(s): 42.60.Fc, 42.55.Wd, 42.60.By, 42.65.Yj

I. INTRODUCTION

Mode-locked lasers have been developed in a wide variety of cavity configurations [1–3]. The fundamental physical mechanism responsible for generating stable mode-locked pulse streams—i.e., saturable absorption [4–6], polarization rotation [7–11], nonlinear interferometry [12–16], active modulation [17,18], or nonlinear mode-coupling [19–22]—can be significantly different in the various cavity configurations. Common to each mode-locked laser, however, is the intensity discrimination which is achieved by the mode-locking mechanism. The intensity discrimination preferentially attenuates low-intensity portions of a pulse with respect to higher-intensity portions. When combined with the laser cavity saturable gain, chromatic dispersion, and self-phase modulation, stable mode-locking operation may be achieved. In this paper, we propose a method for achieving the required intensity discrimination in the cavity. Specifically, we show that the intensity-dependent phase rotation in the laser cavity in combination with phase-sensititive amplification, which acts as a phase filter, can generate and support stable mode-locked pulses. The resulting mode-locked solutions are solitonlike pulses that are locked in phase to the pump phase of the phase-sensitive amplifier. The amplifier, via the pump phase, thus acts to provide both the intensity discrimination required of mode-locking in conjunction with a stabilization mechanism for the generated solitonlike pulses.

Three effects are critical in the mode-locking process. First is the equilibration of energy in the laser which is provided by the saturating cavity gain (e.g., erbium-doped amplifiers). Second is the intensity discrimination which must occur in order for the cavity energy to begin pulse formation or localization. And finally, the onset of pulse formation ultimately leads to soliton generation as a result of the balance of the cavity chromatic dispersion and self-phase modulation [1,3]. These three physical processes are common to mode-locked lasers operating in the anomalous dispersion regime. The effect which changes most from one mode-locked laser to the next is the mechanism responsible for the intensity discrimination. The laser cavity configurations listed above [4–22] have a variety of different physical mechanisms providing an intensity-dependent effect. Here, both energy equilibrization and intensity discrimination can be achieved in a phase-sensitive amplifier (PSA). Essentially, the PSA sifts out and stabilizes the specific mode-locked pulse which has a phase rotation over a cavity round-trip which is commensurate with the pump field driving the PSA. All other phase components are attenuated since they are not in phase with the amplifier. PSAs are an experimentally viable technology which have been developed in the context of a variety of applications including long-haul communications, optical storage, and pulsed optical parametric oscillation [26–34]. Thus the proposal for a PSA mode-locking device considered here relies on standard mode-locked fiber lasers with well-documented PSA technologies.

In principle, this mode-locking mechanism is identical to the phase selection mechanism generated by a figure-8 laser [12–16] and with the nonlinear-polarization rotation-selection mechanism [35,36], which is used in laser cavities mode-locked by a passive polarizer [7–10]. For both these lasers, averaging methods demonstrate the key role that phase selection plays in driving the dynamics of the figure-8 laser [16] and the polarization-rotation laser [11]. In these lasers, the effective phase-selection mechanism is driven by nonlinear processes—i.e., nonlinear phase rotation for the figure-8 laser and nonlinear polarization rotation for the passive polarizer laser. In contrast, the phase selection here is directly accomplished by the linear amplification in the PSA. In any of these situations, an effective intensity discrimination is generated that is necessary for successful mode-locking.

The paper is outlined as follows: Section II gives a qualitative description of the phase-sensitive amplifier and its principle of operation in the mode-locked laser cavity. This is followed by Sec. III, which presents the governing evolution equations in the optical fiber and phase-sensitive amplifier. To make further analytic progress, Sec. IV characterizes the mode-locking dynamics by deriving an averaged model which accounts for the long-time behavior in the laser cavity. The theoretical predictions and conjectures are confirmed in Sec. V with numerical simulations of the mode-locking dynamics using phase-sensitive amplification. A brief summary and review of the mode-locking results are given in Sec. VI.

*kutz@amath.washington.edu

II. PRINCIPLE OF OPERATION

To be more precise about mode-locking with a phase-sensitive amplifier, we consider the basic propagation in a cavity dominated by chromatic dispersion and Kerr nonlinearity. Specifically, we consider the underlying wave propagation governed by the nonlinear Schrödinger (NLS) equation [1]

$$i\frac{\partial Q}{\partial Z}+\frac{1}{2}\frac{\partial^2 Q}{\partial T^2}+|Q|^2Q=0, \tag{1}$$

where the scalings will be discussed below. The NLS equation has the localized soliton solution which takes the form

$$Q(Z,T)=\eta\,\mathrm{sech}(\eta T)\exp(i\eta^2 Z/2). \tag{2}$$

Of note in this solution is the parameter η, which corresponds to an amplitude invariance of the governing NLS equation (1). Thus different amplitudes have a phase-rotation rate given by

$$\Omega=\frac{\eta^2}{2}. \tag{3}$$

This intensity-dependent phase dynamics (2) and (3) is critical for establishing an intensity-discrimination element in the laser cavity via the phase-sensitive amplifier.

The amplification of electromagnetic energy in the phase-sensitive amplifier occurs by amplifying (attenuating) pulse components which are in phase (out of phase) with the pump field of the amplifier. When considering the amplification of a soliton pulse such as Eq. (2), the state of phase of the soliton pulse upon amplification becomes crucial; i.e., in-phase solitons are amplified while out-of-phase solitons are attenuated. The soliton phase relative to the pump phase then determines the behavior the laser cavity dynamics. Again, analogy should be made here with an equivalent effect that occurs in a cavity with a passive polarizer [7–10]. In such a system, it is the nonlinear polarization rotation and its relative relation to the passive polarizer which determines the intensity-selection mechanism for generating the mode-locking behavior [35,36]

Thus the solitons which experience maximal gain are those that after every round-trip are aligned in phase with the pump field of the PSA. This specific soliton is characterized by a particular value of the parameter η in Eq. (2) since it controls the phase-rotation rate Eq. (3). Solitons with η above or below this particular value experience a net attenuation in the cavity due due to their misalignment in phase with the pump. Thus a specific soliton (with associated η value) emerges as a stable attractor in the mode-locked laser cavity.

A schematic of the mode-locked laser configuration is given in Fig. 1. Here the combination of fiber propagation and PSA amplification is given for a ring laser cavity. The total phase accumulated over a single cavity round-trip is given by the rotation rate Ω in Eq. (3) multiplied by the cavity round-trip distance Z_R. Thus the accumulated phase is ΩZ_R. During a single-round trip of the cavity, the pump field

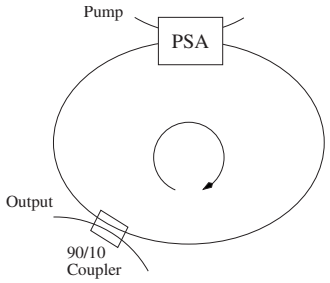

FIG. 1. Proposed experimental arrangement of the laser cavity. The ring configuration includes a phase-sensitive amplifier (PSA) for energy equilibration and intensity discrimination. An output coupler is used to tap off the mode-locked pulse train. In addition to what is shown, it may be advantageous to include an isolator in the cavity as well as an erbium-doped fiber section for augmenting the gain. Recall that the PSA element is primarily used to provide the intensity discrimination for mode-locking.

in the PSA will have experienced a phase rotation of $\Delta\Omega_p$. For in-phase amplification to occur, $\Omega Z_R=\Delta\Omega_p+2n\pi$ with n=integer, which using (3) gives

$$\eta=\sqrt{\frac{2\Delta\Omega_p}{Z_R}} \tag{4}$$

as the specific amplitude which is in phase with the amplifier. It is the soliton of this amplitude which is stabilized and attracted by the laser cavity. Note the critical dependence on $\Delta\Omega_p/Z_R$. The basin of attraction for this specific soliton determines whether the laser has the potential to self-start. Regardless, the phase-selection mechanism clearly provides a Kerr-lens effect [37] which can be used for mode-locking.

The phase-filtering aspect of the PSA has been exploited previously in the context of optical fiber communication systems subject to in-line amplification with PSAs [26–32] in a soliton storage loop [33] and in a pulsed optical parametric oscillator [34]. To a certain extent, the application of the PSAs used in these physical settings is very close to the mode-locking ideas presented here. Thus the PSA as a soliton stabilization mechanism is understood [30–34]. Here, the focus is on generating the soliton from initial white-noise fluctuations in the laser cavity—i.e. mode-locking.

III. GOVERNING EQUATIONS

The theoretical model for the dynamic evolution of electromagnetic energy in the laser cavity is composed of two components: the optical fiber and the PSA element. Each of these critical components are addressed in the following two subsections. Note that since the PSA element is primarily being used to generate intensity discrimination, the general model considered also includes the effects of saturating gain from—for instance, additional erbium-doped amplification.

A. Fiber propagation

The pulse propagation in a laser cavity is governed by the interaction of chromatic dispersion, self-phase modulation, linear attenuation, and bandwidth-limited gain. For conve-

nience, we consider an optical fiber laser such as depicted in Fig. 1. The cavity propagation is given by

$$i\frac{\partial Q}{\partial Z}+\frac{1}{2}\frac{\partial^2 Q}{\partial T^2}+|Q|^2Q+i\gamma Q-ig(Z)\left(1+\tau\frac{\partial^2}{\partial T^2}\right)Q=0, \tag{5}$$

where

$$g(Z)=\frac{2g_0}{1+\|Q\|^2/e_0} \tag{6}$$

and Q represents the electric field envelope normalized by the peak field power $|Q_0|^2$. Here the variable T represents the physical time in the rest frame of the pulse normalized by $T_0/1.76$, where $T_0=200$ fs is the typical full width at half maximum of the pulse. The variable Z is scaled on the dispersion length $Z_0=(2\pi c)/(\lambda_0^2\bar{D})(T_0/1.76)^2$ corresponding to an average anomalous cavity dispersion $\bar{D}\approx 12$ ps/(km nm). This gives the one-soliton peak field power $|Q_0|^2=\lambda_0 A_{\text{eff}}/(4\pi n_2 Z_0)$. Further, $n_2=2.6\times 10^{-16}$ cm^2/W is the nonlinear coefficient in the fiber, $A_{\text{eff}}=60$ μm^2 is the effective cross-sectional area, $\lambda_0=1.55$ μm is the free-space wavelength, c is the speed of light, and $\gamma=\Gamma Z_0$ ($\Gamma=0.2$ dB/km) is the fiber loss. The bandwidth-limited gain in the fiber is incorporated through the dimensionless parameters g and $\tau=(1/\Delta\omega^2)(1.76/T_0)^2$. For a gain bandwidth which can vary from $\Delta\lambda=20$ to 40 nm, $\Delta\omega=(2\pi c/\lambda_0^2)\Delta\lambda$ so that $\tau\approx 0.08-0.32$. The parameter τ controls the spectral gain bandwidth of the mode-locking process, limiting the pulse width.

Finally, it should be noted that a solid-state configuration can also be used to construct the laser cavity. As with optical fibers, the solid-state components of the laser can be engineered to control the various physical effects associated with Eq. (5). Given the robustness of the mode-locking observed, the theoretical and computational predictions considered here are expected to hold for the solid-state configuration.

B. Phase-sensitive amplifier

Modeling of the phase-sensitive amplifier can occur on several levels. The most general model includes the spatiotemporal dynamics of the pump, signal, and idler fields. Included in this description is the parametric, nonlinear interaction of the fields with chromatic dispersion and temporal walk-off due to group-velocity mismatches. The governing equations in this general model are given by [23,24]

$$i\frac{\partial u}{\partial \xi}+\frac{d_u}{2}\frac{\partial^2 u}{\partial T^2}+\chi_u^{(2)}wv^*=0, \tag{7a}$$

$$i\left(\frac{\partial v}{\partial \xi}+v_{vu}\frac{\partial v}{\partial T}\right)+\frac{d_v}{2}\frac{\partial^2 v}{\partial T^2}+\chi_v^{(2)}wu^*=0, \tag{7b}$$

$$i\left(\frac{\partial w}{\partial \xi}+v_{wu}\frac{\partial w}{\partial T}\right)+\frac{d_w}{2}\frac{\partial^2 w}{\partial T^2}+\chi_w^{(2)}uv=0, \tag{7c}$$

where u, v, and w represent the normalized signal, idler, and pump fields, respectively. As with Eq. (5), the variable T represents the physical time in the rest frame of the signal pulse normalized by $T_0/1.76$, where $T_0=200$ fs is the typical full width at half maximum of the pulse. The variable ξ is scaled on the typical phase-sensitive amplifier length $Z_a=5$ mm. The parameter $d_p=(Z_a/T_0^2)d^2k_p/d\omega_p^2$ measures the chromatic dispersion in the signal ($p=u$), idler ($p=v$), and pump ($p=w$) fields where k_p is the wave number and ω_p the frequency. The nonlinear parametric coupling is given by the parameter $\chi_p^{(2)}=(\omega_p^2/2k_pc^2)Q_0Z_a\chi^{(2)}$, where $\chi^{(2)}$ is the nonlinear susceptibility of the amplifying medium, c is the speed of light, and Q_0 is the amplitude scaling used in Eq. (5). Finally the parameter $v_{pq}=dk_p/d\omega_p-dk_q/d\omega_q$ measures the group-velocity walk-off which occurs between the signal, idler, and pump fields.

The governing model (7) has been well studied [23,24] and its phase-sensitive amplification properties well documented [25]. A simplified understanding of the system occurs when two major physical assumptions are made: the system is degenerate so that the signal and idler fields are commensurate, and the PSA crystal is sufficiently short (e.g., 5 mm) so that chromatic dispersion and group-velocity mismatch can be ignored. This reduces the governing evolution equations (7) to the coupled differential equation system [25]

$$i\frac{\partial u}{\partial \xi}+\chi_u^{(2)}wu^*=0, \tag{8a}$$

$$i\frac{\partial w}{\partial \xi}+\chi_w^{(2)}u^2=0. \tag{8b}$$

These equations characterize the fundamental parametric interaction between the degenerate signal and pump fields.

The final simplification which can be made occurs in the undepleted pump approximation. Assuming the pump field to be of much larger in magnitude than the signal field results in

$$i\frac{\partial u}{\partial \xi}+\chi_u^{(2)}wu^*=0, \tag{9a}$$

$$i\frac{\partial w}{\partial \xi}=0, \tag{9b}$$

which has the analytic signal field solution of the form

$$u(\xi,T)=u(0,T)\cosh(\beta\xi)+\exp[i\phi(\xi)]u^*(0,T)\sinh(\beta\xi), \tag{10}$$

where $\beta=\chi_u^{(2)}|w|$ and $\exp[i\phi(\xi)]=iw/|w|$ gives the phase of the pump field. The quadrature decomposition

$$u(0,T)=(A+iB)\exp[i\phi/2] \tag{11}$$

elucidates the nature of the phase-sensitive amplification. In particular, the decomposition (11) shows that the in-phase quadrature component A is amplified while the out-of-phase quadrature component is attenuated since

$$u(\xi,T)=A\exp(\beta\xi)+iB\exp(-\beta\xi). \tag{12}$$

This fundamental behavior in the PSA is key to its use as the intensity discrimination element in the laser cavity. Specifically, only soliton pulses of the form (2) which are aligned

in-phase with the quadrature A persist. Thus a soliton in the cavity must lock to the PSA pump phase in order to persist.

IV. AVERAGED MODE-LOCKING MODEL

The quadrature decomposition (11) suggests a reformulation of the laser cavity equations into in-phase and out-of-phase components. This has been done previously in the context of optical fiber communication systems subject to in-line amplification with PSAs [30–32]. To begin, the governing propagation field $Q(Z,T)$ in Eq. (5) is decomposed into its quadrature components:

$$Q(Z,T) = [A(Z,T) + iB(Z,T)]\exp(i\phi/2). \tag{13}$$

Recall that the PSA amplifies components which are in phase (A) with the amplifier and attenuate those which are out of phase (B) so that

$$Q_+ = [A_- \exp(\alpha) + iB_- \exp(-\alpha)]\exp(i\phi/2). \tag{14}$$

Here the $\pm$ denotes the input field before and after an amplifier, α is the field gain of the amplifier, and ϕ is the reference phase associated with the PSA pump field. Thus the in-phase portion is amplified and the out-of-phase portion is attenuated. This attenuation of the out-of-phase portion works to eliminate phase variations across the signal pulse's profile, which in turn leads to its enhanced stability [30–32].

For convenience, the averaging will assume that all the gain in the system comes from the PSA. Thus the pulse propagation through an optical fiber, which includes dispersion, nonlinearity, linear loss, and periodic phase-sensitive amplification, is governed by the perturbed NLS equation [30,31]

$$i\frac{\partial Q}{\partial Z} + \frac{1}{2}\frac{\partial^2 Q}{\partial T^2} + |Q|^2 Q + i\frac{\Gamma}{\epsilon}Q - i\frac{1}{\epsilon}h\left(\frac{Z}{\epsilon}\right)Q - i\frac{1}{\epsilon}e^{i\phi(Z)}f\left(\frac{Z}{\epsilon}\right)Q^* = 0, \tag{15}$$

where Γ is the linear loss rate in the fiber and the rapidly varying periodic functions h and f account for the effect of the cavity PSA. Specifically, they take the form

$$h(\zeta)Q = [\cosh(\beta|P|z_a) - 1]\sum_{n=1}^{N}\delta(\zeta - nl)Q(nl^-,T), \tag{16}$$

$$f(\zeta)Q^* = \sinh(\beta|P|z_a)\sum_{n=1}^{N}\delta(\zeta - nl)Q^*(nl^-,T). \tag{17}$$

Here z_a is length of the PSA, l is the laser cavity length in terms of $\zeta = Z/\epsilon$, P is the pump amplitude, β is a real constant which depends upon the $\chi^{(2)}$ nonlinearity of the amplifying medium and frequency of the mode-locked signal, and N is the total number of round-trips in the laser cavity. The phase of the amplifier is represented by $\phi(Z)$ and the scalings are those used in Eq. (5). Here the amplifier spacing (cavity length) Z_l is assumed to be much shorter than the dispersion length Z_0 so that $\epsilon \equiv Z_l/Z_0 \ll 1$ [30,31].

Performing a multiple-scale averaging [38] of Eq. (15) using the short length scale ζ, the dispersion length scale Z and the long length scale $\bar{\xi} = \epsilon Z$ give the following fourth-order evolution equation that governs the mode-locking dynamics [30,31]:

$$\frac{\partial U}{\partial \xi} + \frac{1}{4}\left(\frac{\partial^2}{\partial T^2} - \kappa\right)^2 U - \Delta\alpha U - \kappa U^3 + U^5 + 3\beta U\left(\frac{\partial U}{\partial T}\right)^2 + (\beta + 1)U^2\frac{\partial^2 U}{\partial T^2} = 0, \tag{18}$$

where $\beta = (2 - \tanh\Gamma/\Gamma)$, $\kappa = d\phi/dZ$, $\xi = \bar{\xi}/(2\tanh\Gamma)$, $\Delta\alpha$ is an $O(\epsilon^2)$ correction to the exact balance between loss and gain in the laser cavity, and U is the scaled in-phase component of the pulse envelope after each amplifier: namely,

$$U = \left(\frac{1 - e^{-2\Gamma}}{2\Gamma}\right)^{1/2}\mathrm{Re}(Qe^{-i\phi/2}). \tag{19}$$

Equation (15) is a fourth-order, nonlinear, diffusion equation which governs the pulse dynamics over the long length scale ξ. The parameter κ, which represents a constant amplifier phase rotation rate ($\kappa = d\phi/dZ$), can be taken to be unity without loss of generality since it can be scaled out of Eq. (18). Therefore, $\kappa = 1$ in what follows. The amplitude rescaling corresponds to normalizing the pulse envelope so that $\int U^2 dT$ is the average pulse energy over one cavity period [30,31]. Although the evolution equation (18) inherits much of its structure from the NLS equation, it is important to note that the evolution is of a non-Hamiltonian nature and, therefore, its dynamics are those of a dissipative system.

An idea of the general structure of the solutions to Eq. (18) can be obtained by considering $\Gamma = 0$. In this limit,

$$U_0 = \eta\,\mathrm{sech}\,\eta T, \tag{20}$$

where $\eta = [1 \pm 2(\Delta\alpha)^{1/2}]^{1/2}$. The limit of small Γ and $\Delta\alpha$ corresponds physically to assuming that both the amplifier spacing and the amount of overamplification are small. The stability of these solutions can be determined by letting $\delta = \Gamma^2 \ll 1$ and expanding $U = U_0 + \delta U_1 + \delta^2 U_2 + \cdots$ and $\Delta\alpha = \delta\alpha_1 + \delta^2\alpha_2 + \cdots$. Inserting this into Eq. (18) gives

$$U_{0\xi} + L_-^2 U_0 + \delta[U_{1\xi} + L_-L_+U_1 - H_1(U_0,\alpha_1)] + \delta^2[U_{2\xi} + L_-L_+U_2 - H_2(U_0,U_1,\alpha_1,\alpha_2)] + \cdots = 0, \tag{21}$$

where H_n represents the perturbing terms at $O(\delta^n)$ which appear in the equation for U_n and the operators $L_- = -(1/2)\partial_T^2 - U_0^2 + 1/2$ and $L_+ = -(1/2)\partial_T^2 - 3U_0^2 + 1/2$ are the real and imaginary parts of the linearized NLS equation [39]. The self-adjoint operators L_+ and L_- are well understood [39]. It can be proven that the solution (20) is stable for $0 < \Delta\alpha < 1/4$. This then represents the mode-locking regime of interest. Further, is provides analytic proof for the stability of the mode-locking process.

V. MODE-LOCKING DYNAMICS

Numerical simulations of the governing equations are performed to demonstrate the mode-locking dynamics with a PSA. In these simulations, the PSA is used as the intensity

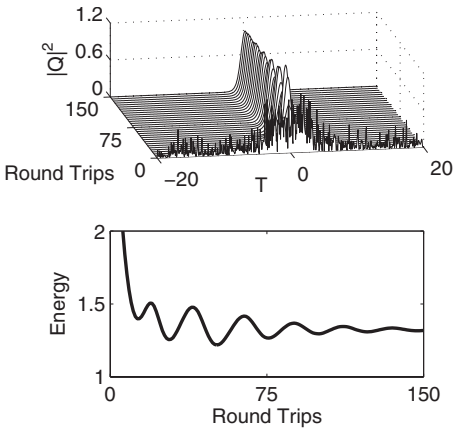

FIG. 2. Laser cavity dynamics showing the formation of a stable mode-locked pulse over approximately 100 round-trips of the cavity. The top figure shows the evolution of the intensity starting from a white-noise initial condition with a small localized peak around $T=0$. The bottom figure shows the relaxation of the energy to the steady-state, mode-locked value. Here $g_0=0.15$, $\Omega_p=\pi/8$, $|w(0,T)|=0.7$, $\tau=0.1$, $e_0=1$, and a 10% output coupling is assumed.

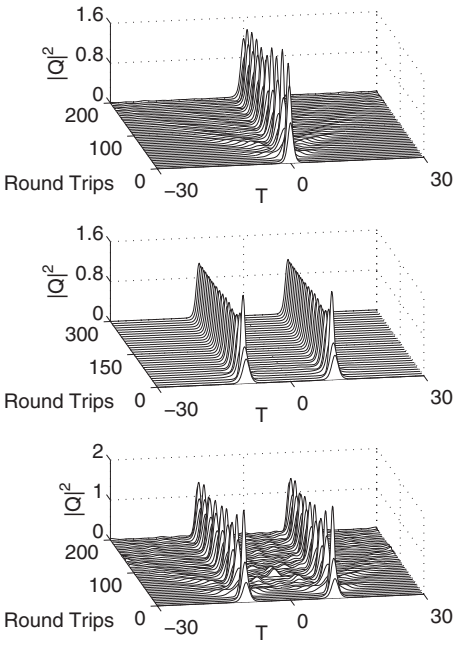

FIG. 3. Mode-locking dynamics as a function of increasing gain pumping from $g_0=0.3$ and 0.35 to 0.5. As g_0 is increased beyond that shown in Fig. 2, the pulse undergoes a Hopf bifurcation to a breathing solution shown in the top panel. Further increasing g_0 gives a stable, two-pulse per round-trip configuration as shown in the middle panel. This also undergoes a Hopf bifurcation to two breather solutions for g_0 increasing further. Although only 200 round-trips are shown, the breathing states persist indefinitely. Here $\Omega_p=\pi/8$, $|w(0,T)|=0.7$, $\tau=0.1$, $e_0=1$, and a 10% output coupling is assumed.

discrimination element by providing phase-locking via the PSA pump field. Additional saturated gain is provided by erbium-doped amplification. The two subsections present simulations first of the full laser cavity dynamics governed by Eq. (5) with Eq. (8) applied every round-trip of the laser cavity and, second, of the average cavity evolution dynamics (18). Both show stability of the mode-locked pulse solution. For all simulations, the numerical integration uses a filtered pseudospectral method in the spatial variable (T) and a fourth-order Runge-Kutta to step forward in the time variable (Z).

A. Full model

To demonstrate the mode-locking dynamics which can occur in the laser cavity, Eq. (5) is simulated with Eq. (8) applied every round-trip of the laser cavity. The scalings used in Eq. (5) give a typical value of $\tau=0.1$ (e.g., 20–30 nm gain bandwidth). We further assume $e_0=1$ and $\gamma=0.1$ and consider a 10% output coupling. The gain parameter g_0 is adjusted to overcome the output coupling losses and cavity attenuation. Note that in this scenario, the PSA is used primarily as a phase-selection mechanism as the overall gain is augmented by erbium-doped amplification.

A critical parameter for mode-locking is the value of Ω_p which denotes the phase rotation experienced by the PSA pump field over one round-trip of the cavity. For the simulations presented here we consider $\Omega_p=\pi/8$. For any specific value chosen, care must then be taken to adjust the remaining free parameters to put the laser cavity in a mode-locking regime. Most notably, the cavity length must be carefully selected due to the soliton-locking condition (4). The initial amplitude of the pump field at the injection into the PSA is $|w(0,T)|=0.7$; i.e., the pump field is a cw beam. The initial pump phase at the first cavity round-trip is zero, and it advances by $\Omega_p=\pi/8$ every round-trip. This is the phase that the mode-locked solution locks to. The PSA is simulated for $\xi=1$ (e.g., ≈ 5 mm) with $\chi_u^{(2)}=\chi_w^{(2)}=0.1$. The propagation in the fiber occurs at $Z=0.5$ (e.g., ≈ 1 m).

The basic mode-locking process is exhibited in Fig. 2 for $g_0=0.15$. Here, white-noise initial data are considered with a small bump centered in the time domain so as to mode-lock the pulse in the center of the computational domain. The bottom panel shows that within approximately 100 round-trips, the laser cavity has settled to the mode-locked pulse solution which is locked in phase with the pump field on a cavity round-trip basis. The bottom panel of Fig. 2 demonstrates the equilibration of energy in the laser cavity from the saturating gain. This is the proof of the concept that mode-locking is possible with a PSA within some physically realizable parameter regime.

Figure 3 demonstrates the mode-locking behavior as the gain pumping parameter g_0 is increased. In the series of plots presented here, the mode-locking first undergoes a Hopf bifurcation (instability) to a breathing pulse solution exhibited in the top panel of Fig. 3. This breathing pulse persists as a stable mode-locked solution. Further increasing g_0 allows for a multipulse scenario in which two pulses per round-trip of the cavity are supported. Further increasing the gain shows these two pulses to undergo a Hopf bifurcation again until a three-pulse scenario is reached. This transition to multipulsing behavior is standard in mode-locked lasers and can be characterized theoretically [40]. Thus the model exhibits one of the common features of a broad range of mode-locked lasers.

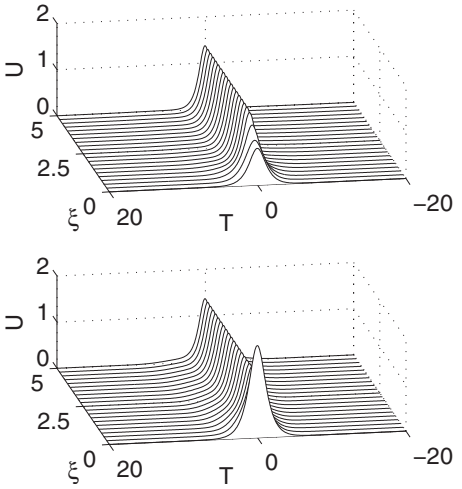

FIG. 4. Mode-locking dynamics as governed by the averaged evolution equation (18). As predicted from the stability analysis, the solution settles exponentially to the steady-state hyperbolic secant solution for initial data with lower amplitude (top panel) or higher amplitude (bottom panel) than the mode-locked solution. Here $\Delta\alpha=0.1$, $\kappa=1$, and $\beta=1$.

B. Averaged model

The average model is a valuable approximation as it clearly relates to the fact that stability is achieved for the hyperbolic secant solutions. Further, the average model holds provided the periodic PSA amplification, or phase-locking, occurs on a scale much shorter than the dispersion length. The simulations presented in the previous subsection confirm this fact. Thus the model gives insight into the possible operating regimes of the laser.

The dynamics of the solitary wave solutions are exhibited in Fig. 4. The stable evolution is demonstrated for the parameter $\gamma=0.1$. In this case, the hyperbolic secant solution is predicted to be exponentially stable. Indeed, the initial conditions are observed to settle quickly to the final steady-state, hyperbolic secant solution. Below a critical amplitude, however, the solutions decay to zero. The stability region for these solutions was explored in detail elsewhere [32,41]. Thus the averaged model suggests that a critical level of initial energy (amplitude) in the cavity is necessary to induce mode-locking. Simulations of the full governing equations as in the last section also confirm this fact. As a consequence, one might expect that significant gain pumping may be required to initially mode-lock the cavity. Alternatively, self-starting may not be as robust as in other mode-locking models.

For values of $\gamma>1/4$, the solitary wave solutions destabilize as eigenvalues cross into the right half-plane. The dynamics in this case leads to the formation of periodic wave trains which can have complicated structures. Figure 5 demonstrates the onset of instability for $\gamma=0.5$ and $\gamma=3$. As in the last section, the additional cavity energy leads to multipulsing behavior. However, the averaged model does not included the effect of gain saturation at its leading order and thus the cavity energy exhibited in Fig. 5 continues to grows as the cavity is filled with pulses. A more detailed description

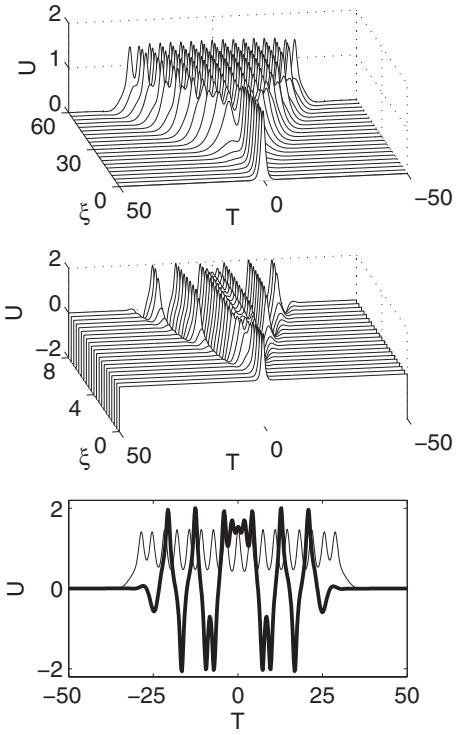

FIG. 5. Instability of the mode-locked solution as $\Delta\alpha$ is increased beyond the predicted stability value of $1/4$. As with the full governing model of the last subsection, a multipulsing instability is observed. However, the averaged model does not include the effects of gain saturation so that the continuous generation of new pulses is observed. For $\Delta\alpha=0.5$ (top panel), a wave train is generated with no nodes as observed from the final state of the system (bottom panel, light line). With $\Delta\alpha=3$ (middle panel), a wave train with nodal separation is created as observed from the final state of the system (bottom panel, bold line).

of the spatial-temporal dynamics of this system which explores a larger class of solutions and their stability is considered by Hewitt and Kutz [42].

VI. CONCLUSIONS

This paper has demonstrated that phase-sensitive amplification can be used as an intensity-discrimination element in a laser cavity for generating stable and robust mode-locking. The intensity-dependent phase rotation of the solitonlike pulse propagating in the laser cavity locks to the phase of the PSA pump phase. Thus a phase filter is effectively created which allows only a specific pulse intensity to persist in the laser cavity: i.e., the mode-locked pulse. The operation of the laser is analogous in concept to the intensity-dependent polarization rotation of laser cavities mode-locked with a passive polarizer.

Numerical simulations of the laser cavity demonstrate the stable, self-starting mode locking with PSAs. Increasing the cavity gain pumping shows that the mode-locked solutions undergo a Hopf bifurcation to a breathing state before stable multipulse operation is established. The transition from N to $N+1$ pulses in the cavity is a commonly observed phenomena in mode-locking models. These results again allow one

to think of the mode-locking with a PSA as generating much of the same behavior observed in a wide variety of laser cavities.

In addition to simulations, a theoretical treatment is given to the stability of the mode-locked pulses in the context of an average model which accounts for the effect of the PSA as a continuous versus discrete effect. The averaged model shows that hyperbolic secant solutions exist and are exponentially stable for a range of physically relevant parameters. Further, the model predicts when instability occurs and how this instability is manifest in the system. The asymptotic validity of the averaged model also lends insight into the expected configurations where the PSA-based mode-locked laser can operate. Specifically, application of the PSA must occur rapidly enough (on a scale shorter than the cavity dispersion length) so that the phase-locking can occur.

ACKNOWLEDGMENT

The author acknowledges support from the National Science Foundation (Grant No. DMS-0604700).

[1] H. A. Haus, IEEE J. Sel. Top. Quantum Electron. **6**, 1173 (2000).
[2] I. N. Duling III and M. L. Dennis, *Compact Sources of Ultrashort Pulses* (Cambridge University Press, Cambridge, U.K., 1995).
[3] J. N. Kutz, SIAM Rev. **48**, 629 (2006).
[4] F. X. Kärtner and U. Keller, Opt. Lett. **20**, 16 (1995).
[5] B. Collings, S. Tsuda, S. Cundiff, J. N. Kutz, M. Koch, W. Knox, and K. Bergman, IEEE J. Sel. Top. Quantum Electron. **3**, 1065 (1998).
[6] S. Tsuda, W. H. Knox, E. A. DeSouza, W. J. Jan, and J. E. Cunningham, Opt. Lett. **20**, 1406 (1995).
[7] K. Tamura, H. A. Haus, and E. P. Ippen, Electron. Lett. **28**, 2226 (1992).
[8] H. A. Haus, E. P. Ippen, and K. Tamura, IEEE J. Quantum Electron. **30**, 200 (1994).
[9] M. E. Fermann, M. J. Andrejco, Y. Silberberg, and M. L. Stock, Opt. Lett. **29**, 447 (1993).
[10] D. Y. Tang, W. S. Man, and H. Y. Tam, Opt. Commun. **165**, 189 (1999).
[11] H. Leblond, M. Salhi, A. Hideur, T. Chartier, M. Brunel, and F. Sanchez, Phys. Rev. A **65**, 063811 (2002).
[12] I. N. Duling, Electron. Lett. **27**, 544 (1991).
[13] D. J. Richardson, R. I. Laming, D. N. Payne, V. J. Matsas, and M. W. Phillips, Electron. Lett. **27**, 542 (1991).
[14] M. L. Dennis and I. N. Duling, Electron. Lett. **28**, 1894 (1992).
[15] F. O. Ölday, F. W. Wise, and T. Sosnowski, Opt. Lett. **27**, 1531 (2002).
[16] M. Salhi, A. Haboucha, H. Leblond, and F. Sanchez, Phys. Rev. A **77**, 033828 (2008).
[17] F. X. Kärtner, D. Kopf, and U. Keller, J. Opt. Soc. Am. B **12**, 486 (1994).
[18] H. A. Haus, IEEE J. Quantum Electron. **11**, 323 (1975).
[19] J. N. Kutz, *Dissipative Solitons*, Vol. 241 of Lecture Notes in Physics, edited by N. N. Akhmediev and A. Ankiewicz (Springer, Berlin, 2005).
[20] J. Proctor and J. N. Kutz, Opt. Lett. **30**, 2013 (2005).
[21] J. Proctor and J. N. Kutz, Opt. Express **13**, 8933 (2005).
[22] K. Intrachat and J. N. Kutz, IEEE J. Quantum Electron. **39**, 1572 (2003).
[23] G. A. Bukauskas, V. I. Kabelka, A. S. Piskarskas, and A. Yu Stabinis, Sov. J. Quantum Electron. **4**, 290 (1974).
[24] R. Danelyus, G. Dikchyus, V. Kabelka, A. Piskarskas, and A. Stabinis, Sov. J. Quantum Electron. **7**, 1360 (1977).
[25] R. W. Boyd, *Nonlinear Optics*, 2nd ed. (Academic Press, San Diego, CA, 2003).
[26] A. Takada and W. Imajuku, Electron. Lett. **34**, 274 (1998).
[27] M. Vasilyev, Opt. Express **13**, 7563 (2005).
[28] R. Tang, P. Devgan, P. L. Voss, V. S. Grigoryan, and P. Kumar, IEEE Photonics Technol. Lett. **17**, 1845 (2005).
[29] C. J. McKinstrie and S. Radic, Opt. Express **12**, 4973 (2004).
[30] J. N. Kutz, W. L. Kath, P. Kumar, and R. D. Li, Opt. Lett. **18**, 802 (1993).
[31] J. N. Kutz, C. Hile, W. L. Kath, P. Kumar, and R. D. Li, J. Opt. Soc. Am. B **11**, 2112 (1994).
[32] J. N. Kutz and W. L. Kath, SIAM J. Appl. Math. **56**, 611 (1996).
[33] G. D. Bartolini, D. K. Serkland, P. Kumar, and W. L. Kath, IEEE Photonics Technol. Lett. **29**, 1020 (1997).
[34] D. K. Serkland, G. D. Bartolini, A. Agarwal, P. Kumar, and W. L. Kath, Opt. Lett. **23**, 795 (1998).
[35] A. Kim, J. N. Kutz, and D. Muraki, IEEE J. Quantum Electron. **36**, 465 (2000).
[36] K. Spaulding, D. Yong, A. Kim, and J. N. Kutz, J. Opt. Soc. Am. B **19**, 1045 (2002).
[37] T. Brabec, Ch. Spielmann, P. F. Curley, and F. Krausz, Opt. Lett. **17**, 1292 (1992).
[38] C. M. Bender and S. A. Orszag, *Advanced Mathematical Methods for Scientists and Engineers* (McGraw-Hill, New York, 1978).
[39] M. Weinstein, SIAM J. Math. Anal. **16**, 472 (1985).
[40] J. N. Kutz and B. Sandstede, Opt. Express **16**, 636 (2008).
[41] J. C. Alexander, M. G. Grillakis, C. K. R. T. Jones, and B. Sandstede, ZAMP **48**, 175 (1997).
[42] S. E. Hewitt and J. N. Kutz, SIAM J. Appl. Dyn. Syst. **4**, 808 (2005).